Available online at www.sciencedirect.com

ScienceDirect

Procedia Engineering 102 (2015) 1885 – 1889

Procedia Engineering

www.elsevier.com/locate/procedia

The 7th World Congress on Particle Technology (WCPT7)

Synthesis and properties of new multifunctional hexaferrite powders

J. Li[a], H.-F. Zhang[a], G.-Q. Shao[a*], D. Chen[a], G.-G. Zhao[a], Z.-S. Gao[a], J.-H. Liu[a], J.-S. Lu[b], X.-B. Li[b]

[1]*State Key Laboratory of Advanced Technology for Materials Synthesis and Processing, Wuhan University of Technology, Wuhan 430070, China*

[2]*Key Laboratory of Nondestructive Testing of Ministry of Education, Nanchang Hangkong University, Nanchang 330063, China*

Abstract

$Sr_3Co_2Fe_{24}O_{41}$ (Sr_3Co_2Z) hexaferrite has potential applications in spintronics and multiferroics. To synthesize a single-phase Sr_3Co_2Z is very difficult now while the corresponding reaction process lacks investigating. In this work, the reaction mechanism to synthesize Z/W/M-type strontium hexaferrite powders was studied. Results show that the $SrFe_{12}O_{19}$ (SrM) could react with $CoFe_2O_4$ to form $SrCo_2Fe_{16}O_{27}$ ($SrCo_2W$) in the range 750 °C < T < 1150 °C. The $SrCo_2Fe_{16}O_{27}$ ($SrCo_2W$) transforms into Sr_3Co_2Z in the range 1150 °C < T < 1250 °C.

Selection and peer-review under responsibility of Chinese Society of Particuology, Institute of Process Engineering, Chinese Academy of Sciences (CAS)

Keywords: Reaction process; Z-type hexaferrite; spintronics; multiferroic

1. Introduction

Because of high permeability and quality factors (up to 1 GHz), Z-type hexaferrites are usually used as multiplayer chip inductors in the microwave field[1-4]. Their magnetoelectric (ME) property was reported in 2010[5] and since then attracted much attention for their potential applications in spintronics and multiferroics[6-8]. The new multifunctional materials include dual field read-write magnetic memories and data storage, sensors and switches, transducers, active responsive components, controlled or adaptive absorption and resonance of EM fields from RF to MW and GHz, field-tuneable MW components, phase shifters and duplexers *et al.*. The hexaferrites are classified into six types (M, Y, Z, W, X and U) according to different stacking sequences of three fundamental blocks (S-, R- and T-blocks) in their crystal structure. The Z-type hexaferrite is formed according the $RSTSR^*S^*T^*S^*$ sequence (the asterisk indicates those 180° rotated around *c*-axis)[9]. Due to the complex crystal structure, it is very difficult to synthesize a single-phase Z-type hexaferrite. Even some fascinating results of magnetic-electronic coupling in $Sr_3Co_2Fe_{24}O_{41}$ (Sr_3Co_2Z) have been reported since 2010, most of them are found to coexist with M-, W-, U- or Y-type hexaferrites[1, 5].

Raw materials such as metal oxides, carbides[5, 7, 10], metal nitrates, citrates or halides[11-14] have been processed to synthesize Z-type hexaferrites. The sequence of phase formation for a $Ba_3Co_2Fe_{24}O_{41}$ (Ba_3Co_2Z) has been described as: raw materials → M + Y → Z[11, 12, 15]. The optimal temperature range is found within 1200 - 1350 °C (for solid state method) or 1150 - 1200 °C (for wet chemical method). The Sr_3Co_2Z has been synthesized from a sol-gel precursor in 2001[13], via polymerizable complex in 2011[14] and through solid state reaction in 2003 and 2006[16, 17]. Only one work involves a single-phase but lacks the reaction process[14].

Corresponding author. Tel.:+86-13808694306; fax: +64 6 3505241.
E-mail address: shaogangqin@126.com; gqshao@whut.edu.cn

Selection and peer-review under responsibility of Chinese Society of Particuology, Institute of Process Engineering, Chinese Academy of Sciences (CAS)
doi:10.1016/j.proeng.2015.01.327

In this work, the reaction mechanism to synthesize Z/W/M-type strontium hexaferrite powders was studied. The phase form, phase composition and crystallite size were characterized. The relationship of process and phase purity was discussed.

2. Experimental

Target powders were prepared using $SrCO_3$ (99.5$^+$ wt.%), $Co(NO_3)_2{\cdot}6H_2O$ (99.5$^+$ wt.%) and $Fe_2O_3{\cdot}xH_2O$ (99.9$^+$ wt.%) as raw materials, in which the $Fe_2O_3{\cdot}xH_2O$ was pre-obtained by precipitation from $Fe(NO_3)_3{\cdot}9H_2O$ and ammonia. Three raw materials were mixed, ground and then calcined at 800 °C for 4 h in air. After pulverized and well ground, the pre-synthesized powder was divided into five parts and calcined at 900 °C, 1100 °C, 1150 °C, 1200 °C and 1250 °C for 4 h in air, respectively.

The reaction processes were studied by DSC-TG (Netzsch STA 449c/3/G, 5 °C/min) using the mixture of two or three raw materials. $SrCO_3$ and $Co(NO_3)_2{\cdot}6H_2O$ were mixed with the molar ratio of 3 : 2, $Co(NO_3)_2{\cdot}6H_2O$ and $Fe_2O_3{\cdot}xH_2O$ were 1 : 6, $SrCO_3$ and $Fe_2O_3{\cdot}xH_2O$ were 1 : 4, and the tri-mixture was 3 : 2 : 12.

Phase determination was carried out ($10° \le 2\theta \le 80°$) by X-ray diffraction (XRD) using a D8 Advance X-ray diffractometer (Bruker, Germany), with a Cu K_α radiation (λ = 1.54184 Å, 40 kV, 40 mA). By whole-pattern fitting with the JADE software (Materials Data Inc., USA), the phase content and the average size of crystallite were obtained. Reproducibility for Parabolic background parameters, scale factors (where the quantitative phase-composition information was extracted from), structural parameters and profile parameters (Pseudo-Voigt) were considered for refinement until the results converged into minimum values.

3. Results and discussion

3.1. Reaction process

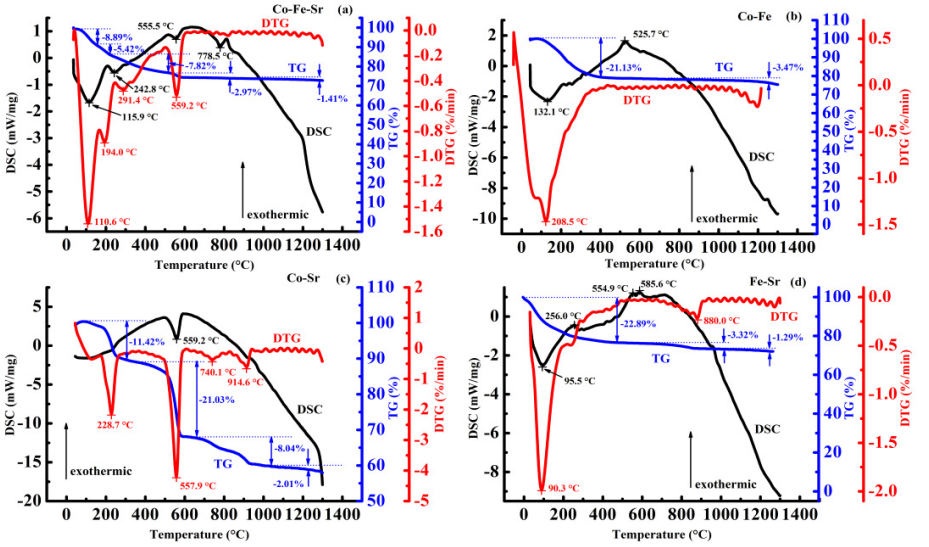

Fig. 1. DSC, TG and DTG profiles for the mixture of raw materials: (a) Co-Fe system; (b) Co-Sr system; (c) Fe-Sr system; (d) Co-Fe-Sr system

Fig. 1 shows the DSC, TG and DTG profiles for the mixture of raw materials.

For the Co-Fe system [Fig. 1(a)], the endothermic peak at 132.1 °C can be attributed to the loss of crystal water from $Fe_2O_3{\cdot}xH_2O$ and $Co(NO_3)_2{\cdot}6H_2O$, considering the DTG's peak at 208.5 °C. The exothermic peak at 525.7 °C is corresponding to the formation of $CoFe_2O_4$, combined the effect of $Co(NO_3)_2$ decomposition to CoO below 330 °C (endothermic)[18].

For the Co-Sr system [Fig. 1(b)], the endothermic peak at ~230 °C can also be attributed to the loss of crystal water from $Fe_2O_3{\cdot}xH_2O$ and $Co(NO_3)_2{\cdot}6H_2O$, considering the DTG's peak at 228.7 °C. The

endothermic peak at 559.2 °C corresponds to $Co(NO_3)_2$ decomposition, which attained the maximum at 740.1 °C (see the peak in DTG curve). The peak in DTG curve at 914.6 °C is attributed to the $SrCO_3$ decomposition. The exothermic peak closed to 1300 °C is corresponding to the formation of Co-Sr-O compound.

For the Fe-Sr system [Fig. 1(c)], the endothermic peaks at 95.5 °C and 256.0 °C are attributed to the loss of crystal water from $Fe_2O_3 \cdot xH_2O$. The exothermic peaks at 585.6 °C corresponds to the formation of Fe-Sr-O compound at the very beginning of $SrCO_3$ decomposition. The exothermic peak closed to 1000 °C corresponds to the formation of $SrFe_{12}O_{19}$ (SrM) while the $SrCO_3$ decomposition attains the maximum at 880.0 °C (see the peak in DTG curve). The ΔG for the reaction $SrO + 6Fe_2O_3 = SrFe_{12}O_{19}$ is calculated to be -68.47 kJ/mol at 711 °C (983 K)[19].

For the Co-Fe-Sr system [Fig. 1(d)], there are two endothermic peaks (115.9 °C and 242.8 °C) with a mass loss of 22.13 wt% below 500 °C, which are attributed to the loss of crystal water from $Fe_2O_3 \cdot xH_2O$ and $Co(NO_3)_2 \cdot 6H_2O$. The endothermic peak at 555.5 °C with a mass loss of 2.97 wt% corresponds to the $Co(NO_3)_2$ decomposition. The exothermic peaks at 800.5 °C and ~1200 °C are corresponding to the formation of $SrCo_2Fe_{16}O_{27}$ ($SrCo_2W$) and $Sr_3Co_2Fe_{24}O_{41}$ (Sr_3Co_2Z), respectively (see the section 3.2).

3.2. Phase analysis

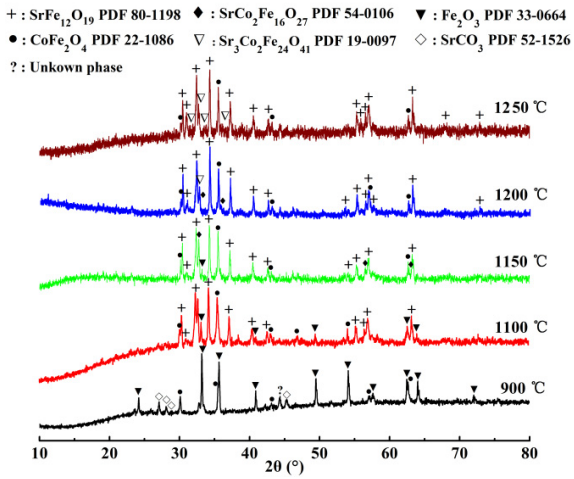

Fig. 2. XRD patterns of powders calcined at various temperatures

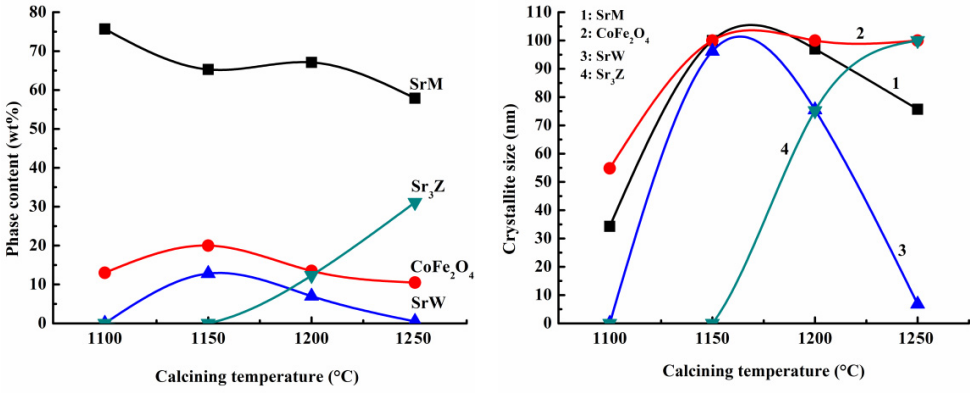

Fig. 3. Phase content (a) and average crystallite size (b) of powders calcined at various temperatures

Fig. 2 is the XRD patterns of powders calcined at different temperatures. The calculated phase

content of SrM, $CoFe_2O_4$, $SrCo_2W$ and Sr_3Co_2Z is shown in Fig. 3(a). The average crystallite size of samples is shown in Fig. 3(b). Results show that $SrCO_3$ (PDF 52-1526) does not decompose completely at 900 °C. The main product at this temperature is $CoFe_2O_4$ (PDF 22-1086), while the residual Fe_2O_3 (PDF 89-0597) exists. The major phase becomes SrM (PDF 80-1198) when the calcining temperature is above 900 °C. $CoFe_2O_4$ always exists in the product in the temperature range investigated. $SrCO_3$ and Fe_2O_3 disappear when the temperature reaches 1100 °C and 1200 °C, respectively. The $SrCo_2W$ attains its maximum phase content at 1150 °C from the reaction between SrM and $CoFe_2O_4$. After 1150 °C, the phase content of $SrCo_2W$ decreases and the Sr_3Co_2Z appears.

At 1150 °C, the SrM, $CoFe_2O_4$ and $SrCo_2W$ attain their maximum crystallite size. The crystallite size of Sr_3Co_2Z increases gradually after 1150 °C, while that of SrM and $SrCo_2W$ decreases. The change in crystallite size for SrM and $SrCo_2W$ during 1150 °C and 1250 °C indicates the following fact: SrM could react with $CoFe_2O_4$ to form $SrCo_2W$ before its growth, and $SrCo_2W$ transforms into Sr_3Co_2Z before its growth.

It can be deduced from the above analysis that the reaction process in this study:

$T < 800$ °C:

$$Co(NO_3)_2 \cdot 6H_2O = CoO + 6H_2O + 0.5O_2 \uparrow + 2NO_2 \uparrow$$

$$Fe_2O_3 \cdot xH_2O = Fe_2O_3 + xH_2O$$

$$CoO + Fe_2O_3 = CoFe_2O_4(S)$$

500 °C < T < 950 °C:

$$SrCO_3 = SrO + CO_2 \uparrow$$

$$SrO + 6Fe_2O_3 = SrFe_{12}O_{19}(SrM)$$

750 °C < T < 1150 °C:

$$SrFe_{12}O_{19}(SrM) + CoFe_2O_4(S) = SrCo_2Fe_{16}O_{27}(SrCo_2W)$$

1150 °C < T < 1250 °C:

$$SrCo_2Fe_{16}O_{27}(SrCo_2W) + 2SrO + 4Fe_2O_3 = Sr_3Co_2Fe_{24}O_{41}(Sr_3Co_2Z)$$

That is: raw materials → S + M → W → Z. This is different as the reported process (raw materials → M + Y → Z[11, 12, 15]), because Y-type hexaferrite of $Sr_2Co_2Fe_{12}O_{22}$ was not detected in this study.

As the intermediate product, SrM plays a key role for the Sr_3Co_2Z formation. The rigorously control is crucial to synthesize a single-phase Sr_3Co_2Z.

4. Conclusion

To synthesize Z/W/M-type strontium hexaferrite powders by using $SrCO_3$, $Co(NO_3)_2 \cdot 6H_2O$ and $Fe_2O_3 \cdot xH_2O$ as raw materials, there is no $Sr_2Co_2Fe_{12}O_{22}$ (Sr_2Co_2Y) detected. The reaction process should be: raw materials → $CoFe_2O_4$ + $SrFe_{12}O_{19}$ (SrM) → $SrCo_2Fe_{16}O_{27}$ ($SrCo_2W$) → $Sr_3Co_2Fe_{24}O_{41}$ (Sr_3Co_2Z). The rigorously control of SrM phase is crucial to synthesize a single-phase Sr_3Co_2Z.

Acknowledgements

The authors gratefully acknowledge Prof. B.-L. Wu in Key Laboratory of New Processing Technology for Nonferrous Metals and Materials (GUT, China). This work was supported by grants from State Key Laboratory of Advanced Technology for Materials Synthesis and Processing (WUT, China) (Grant Nos. 2013-KF-2, 2014-KF-6), and the Open Research Foundation of Key Laboratory of Nondestructive Testing (NHU, China) (Grant No. Zd201329002).

References

[1] W. Gtinberger, B. Springmann, M. Brusberg, M. Schmidt, and R. Jahnke, Rubber bonded ferrite layer as a microwave resonant absorber in a frequency range from 3 up to 16 GHz, J. Magn. Magn. Mater. 101 (1991) 173-174.

[2] O. Kimura, M. Matsumoto, and M. Sakakura, Enhanced dispersion frequency of hot-pressed Z-type magnetoplumbite ferrite with the composition $2CoO \cdot 3Ba_{0.5}Sr_{0.5}O \cdot 10.8Fe_2O_3$, J. Am. Ceram. Soc. 78 (1995) 2857-2860.

[3] K.N. Rozanov, Z.W. Li, L.F. Chen, and M.Y. Koledintseva, Microwave permeability of Co_2Z composites, J. Appl. Phys. 97 (2005) 013905.

[4] M.M. Rashad, H.M. El-Sayed, M. Rasly, A.A. Sattar, and I.A. Ibrahim, Magnetic and dielectric properties of polycrystalline La doped barium Z-type hexaferrite for hyper-frequency applications, J. Mater. Sci.: Mater. Electron. 24 (2013) 282-289.

[5] Y. Kitagawa, Y. Hiraoka, T. Honda, T. Ishikura, H. Nakamura, and T. Kimura, Low-field magnetoelectric effect at room temperature, Nat. Mater. 9 (2010) 797-802.

[6] M. Soda, T. Ishikura, H. Nakamura, Y. Wakabayashi, and T. Kimura, Magnetic ordering in relation to the room-temperature magnetoelectric effect of $Sr_3Co_2Fe_{24}O_{41}$, Phys. Rev. Lett. 106 (2011) 087201.

[7] X. Zhang, Y.G. Zhao, Y.F. Cui, L.D. Ye, J.W. Wang, S. Zhang, H.Y. Zhang, and M.H. Zhu, Magnetodielectric effect in Z-type hexaferrite, Appl. Phys. Lett. 100 (2012) 032901.

[8] K. Okumura, K. Haruki, T. Ishikura, S. Hirose, and T. Kimura, Multilevel magnetization switching by electric field in c-axis oriented polycrystalline Z-type hexaferrite, Appl. Phys. Lett. 103 (2013) 032906.

[9] T. Kimura, Magnetoelectric hexaferrites, Annu. Rev. Condens. Matter Phys. 3 (2012) 93-110.

[10] G.H. Jonker, H.P.J. Wijn, and P.B. Braun, A new class of oxidic ferromagnetic materials with hexagonal crystal structures, Proceedings of the IEE - Part B: Radio and Electronic Engineering. 104 (1957) 249-254.

[11] H. Zhang, J. Zhou, Z. Yue, P. Wu, Z. Gui, and L. Li, Synthesis of Co_2Z hexagonal ferrite with planar structure by gel self-propagating method, Mater. Lett. 43 (2000) 62-65.

[12] R.C. Pullar, S.G. Appleton, M.H. Stacey, M.D. Taylor, and A.K. Bhattacharya, The manufacture and characterisation of aligned fibres of the ferroxplana ferrites Co_2Z, 0.67% CaO-doped Co_2Z, Co_2Y and Co_2W, J. Magn. Magn. Mater. 186 (1998) 313-325.

[13] R.C. Pullar and A.K. Bhattacharya, The synthesis and characterization of the hexagonal Z ferrite, $Sr_3Co_2Fe_{24}O_{41}$, from a sol-gel precursor, Mater. Res. Bull. 36 (2001) 1531-1538.

[14] T. Kikuchi, T. Nakamura, T. Yamasaki, M. Nakanishi, T. Fujii, J. Takada, and Y. Ikeda, Synthesis of single-phase $Sr_3Co_2Fe_{24}O_{41}$ Z-type ferrite by polymerizable complex method, Mater. Res. Bull. 46 (2011) 1085-1087.

[15] L. Jia, Y. Tang, H. Zhang, P. Deng, Y. Liu, and B. Liu, Effects of perovskite additives on the electromagnetic properties of Z-Type hexaferrites, Jap. J. Appl. Phys. 49 (2010) 063001.

[16] Y. Takada, T. Tachibana, T. Nakagawa, T.A. Yamamoto, T. Shimada, and S. Kawano, Estimation of magnetic structures of Z-type ferrites: $(Ba, Sr)_3Co_2Fe_{24}O_{41}$ by neutron diffraction, J. Jpn. Soc. Powder Powder Metallurgy. 50 (2003) 618-625.

[17] Y. Takada, T. Nakagawa, M. Tokunaga, Y. Fukuta, T. Tanaka, T.A. Yamamoto, T. Tachibana, S. Kawano, Y. Ishii, and N. Igawa, Crystal and magnetic structures and their temperature dependence of Co_2Z-type hexaferrite $(Ba,Sr)_3Co_2Fe_{24}O_{41}$ by high-temperature neutron diffraction, J. Appl. Phys. 100 (2006) 043904.

[18] Z.D. Zivkovic, D.T. Zivkovic, and D.B. Grujicic, Kinetics and mechanism of the thermal decomposition of $M(NO_3)_2 \cdot nH_2O$ (M = Cu, Co, Ni), J. Therm. Anal. 53 (1998) 617-623.

[19] S.K. Rakshit, S.C. Parida, S. Dash, Z. Singh, R. Prasad, and V. Venugopal, Thermochemical studies on $SrFe_{12}O_{19}$(s), Mater. Res. Bull. 40 (2005) 323-332.